# Electronic Structure of M($\eta^4$-$P_2C_2Bu^t_2$), where M = Ge, Sn, and Pb: Photoelectron Spectroscopy and Density Functional Studies

Grant Anderson,[†] Jennifer C. Green*,[†] and Matthew D. Francis[‡]

*Inorganic Chemistry Laboratory, University of Oxford, South Parks Road, Oxford OX1 3QR, U.K., and School of Chemistry, Physics and Environmental Science, University of Sussex, Brighton, BN1 9QJ, U.K.*

*Received March 5, 2003*

Density functional calculations are used to optimize the geometry of M($\eta^4$-$P_2C_2R_2$) (M = Ge, Sn, Pb; R = H, $Bu^t$) and examine the orbital structure. He I and He II spectra are reported for M($\eta^4$-$P_2C_2Bu^t_2$) (M = Ge and Sn), and the spectra are assigned. Ionization energy calculations are in good agreement with the experimental values. The binding of the diphosphacyclobutadienyl ring to the metal involves donation from the ring $\pi$ orbital into the metal s, $p_x$, and $p_y$ orbitals. A possible intermediate in the formation of a M($\eta$-$P_2C_2R_2$) complex is presented; this has a $MP_2C_2$ square-pyramidal structure with P at the apex and M in the square base. The transition states for rearrangement to the product, where M is at the apex of a square pyramid, are identified. The reactivity of M($\eta^4$-$P_2C_2R_2$) as a base and toward oxidative addition is explored.



## Introduction

Although the 1,3-diphosphacyclobutadienyl ring has been found to be stabilized by transition metals since 1986,[1−6] it is only recently that this moiety has been shown to form main group metal adducts by the characterization of M($\eta^4$-$P_2C_2Bu^t_2$), where M is a group 14 element, either Ge, Sn, or Pb.[7,8] These compounds have been classified as diphospacyclobutadienyl complexes of the divalent metal, although they may also be regarded as 24-electron *nido*-clusters, having the square-pyramidal framework characteristic of this class.

The synthetic pathway is of interest in that the compounds are formed by reaction of the metal dihalide with [Zr($\eta^5$-$C_5H_5$)$_2$($\eta^2$-$C_2Bu^t_2P_2$)].[8] The P−P bond in the 1,3-diphosphabicyclo[1.1.0]butane ligand is broken, and a four-membered ring is formed, coordinated in an $\eta^4$ fashion to the metal.

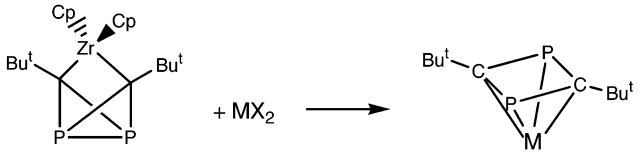


The combination of photoelectron (PE) spectroscopy and density functional (DF) calculations has proved a powerful tool in investigating the electronic structure of both transition metal and main group phosphametallocenes.[9−13] In this work we describe DF calculations on both M($\eta^4$-$P_2C_2Bu^t_2$) and the model compounds M($\eta^4$-$P_2C_2H_2$). PE spectra of M($\eta^4$-$P_2C_2Bu^t_2$) (M = Ge and Sn) are assigned. Rearrangement from a proposed intermediate M($P_2C_2H_2$) to M($\eta^4$-$P_2C_2H_2$) is also examined, and oxidative addition and acid−base reactivity are explored.

## Experimental Section

The compounds M($\eta^4$-$P_2C_2Bu^t_2$) (M = Ge and Sn) were prepared by the literature route.[8]

PE spectra were measured using a Helectros 0078 spectrometer with a He discharge lamp capable of producing both He I and He II spectra. The spectrometer was interfaced with an Atari processor, which enabled spectral acquisition by repeated scans. The samples were held at 40 °C during measurement and were calibrated using He, Xe, and $N_2$. Band intensities were estimated using the Gaussian fitting program available in the IGOR program suite.[14] Band positions and widths were obtained by a free fit to the He I spectra and were maintained at the same IE and proportionate widths for the lower resolution He II spectra.

[†] University of Oxford.
[‡] University of Sussex.

(1) Hitchcock, P. B.; Maah, M. J.; Nixon, J. F. *J. Chem. Soc., Chem. Commun.* **1986**, 737.
(2) Binger, P. B.; Milczarek, R.; Mynott, R.; Regitz, M.; Rösch, W. *Angew. Chem., Int. Ed. Engl.* **1986**, *25*, 644.
(3) Binger, P. B.; Milczarek, R.; Mynott, R.; Krüger, C.; Tsay, Y. H.; Raabe, E.; Regitz, M. *Chem. Ber.* **1988**, *121*, 637.
(4) Dreiss, M.; Hu, D.; Pritzkow, H.; Schäufele, H.; Zenneck, U.; Regitz, M.; Rösch, W. *J. Organomet. Chem.* **1987**, *334*, C35.
(5) Wettling, T.; Wolmershaüser, G.; Binger, P. B.; Regitz, M. *J. Chem. Soc., Chem. Commun.* **1990**, 1541.
(6) Cloke, F. G. N.; Flower, K. R.; Hitchcock, P. B.; Nixon, J. F. *J. Chem. Soc., Chem. Commun.* **1994**, 489.
(7) Francis, M. D.; Hitchcock, P. B. *J. Chem. Soc., Chem. Commun.* **2002**, 86.
(8) Francis, M. D.; Hitchcock, P. B. *Organometallics* **2003**, in press.
(9) Al-Ktaifani, M.; Green, J. C.; Hitchcock, P. B.; Nixon, J. F. *J. Chem. Soc., Dalton Trans.* **2001**, 1726.
(10) Bartsch, R.; Cloke, F. G. N.; Green, J. C.; Matos, R. M.; Nixon, J. F.; Suffolk, R. J.; Suter, J. L.; Wilson, D. J. *J. Chem. Soc., Dalton Trans.* **2001**, 1013.
(11) Clendenning, S. B.; Green, J. C.; Nixon, J. F. *J. Chem. Soc., Dalton Trans.* **2000**, 1507.
(12) Clentsmith, G. K. B.; Cloke, F. G. N.; Francis, M. D.; Green, J. C.; Hitchcock, P. B.; Nixon, J. F.; Suter, J. L.; Vickers, D. M. *J. Chem. Soc., Dalton Trans.* **2000**, 1715.
(13) Cloke, F. G. N.; Green, J. C.; Hanks, J. R.; Nixon, J. F.; Suter, J. L. *J. Chem. Soc., Dalton. Trans.* **2000**, 3534−3536.
(14) *IGOR*, 4.0 ed.; Wavemetrics: Lake Oswego, 2000.

10.1021/om030161m CCC: $25.00 
Publication on Web 06/12/2003

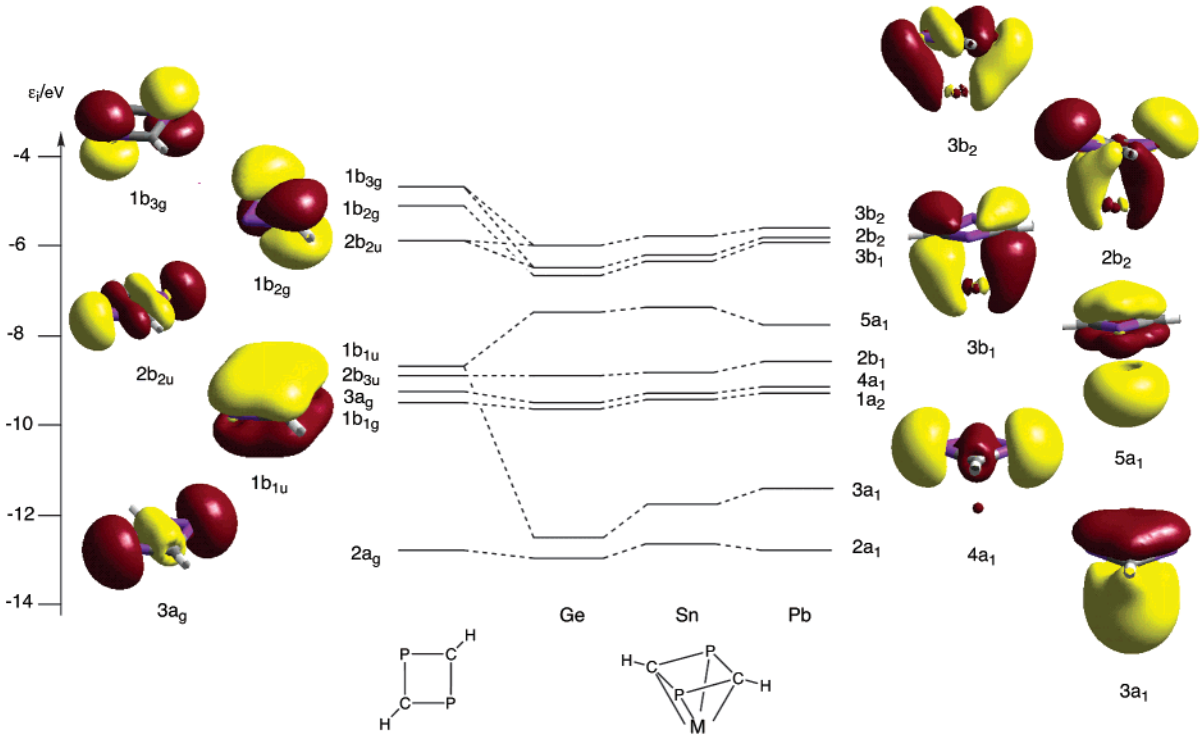


**Figure 1.** MO scheme for M($\eta^4$-$P_2C_2H_2$) showing the relation between the parent orbitals of planar $P_2C_2H_2$ and the MOs for M = Ge, Sn, and Pb. Energies are for neutral fragments. Isosurfaces of key orbitals for $P_2C_2H_2$ and Sn($\eta^4$-$P_2C_2H_2$) are also shown.

Density functional calculations were carried out using the Amsterdam Density Functional program suite ADF 2002.02.[15] Scalar relativistic corrections were included via the ZORA method.[16,17] The generalized gradient approximation was employed, using the local density approximation of Vosko, Wilk, and Nusair[18] together with nonlocal exchange correction by Becke[19] and nonlocal correlation corrections by Perdew.[20] TZ2P basis sets were used with triple-$\zeta$ accuracy sets of Slater type orbitals and two polarization functions added to the main group atoms. The cores of the atoms were frozen up to 1s for C, 2p for P, 3d for Ge, 4d for Sn, and 4f for Pb. Vertical ionization energies (IE) were estimated by calculating the energy of the molecular ions in their ground or excited states with the optimized geometry of the molecule. The IEs were found by the energy differences from that of the parent molecule.

## Results and Discussion

**Electronic Structure.** Geometries were optimized for M($\eta^4$-$P_2C_2R_2$) (M = Ge, Sn, Pb; R = H, Bu$^t$). The results for framework distances and angles are given in Table 1 together with the experimental data, where R = Bu$^t$. The results are in good agreement with the crystal structure data,[7,8] although the M−C and M−P distances show greater variation with M experimentally than they do computationally. There is little variation between the calculated framework distances for R = H and R = Bu$^t$. Thus the R = H compounds provide good simple models for examining the bonding of the ring to the metal.

**Table 1. Calculated Distances (Å) and Angles (deg) for M($\eta^4$-$P_2C_2R_2$) (M = Ge, Sn, Pb; R = H, Bu$^t$) and Experimental Data (*in italics*) for M($\eta^4$-$P_2C_2R_2$) (M = Ge, Sn, Pb; R = Bu$^t$)**

| M, R | M−P | M−C | P−C | C−P−C | P−C−P |
|---|---|---|---|---|---|
| Ge, H | 2.45 | 2.27 | 1.79 | 80 | 99 |
| Sn, H | 2.64 | 2.44 | 1.79 | 81 | 99 |
| Pb, H | 2.67 | 2.48 | 1.79 | 81 | 99 |
| Ge, Bu$^t$ | 2.46 | 2.28 | 1.79 | 82 | 98 |
| | *2.416* | *2.204* | *1.792* | *81.1* | *98.3* |
| Sn, Bu$^t$ | 2.64 | 2.44 | 1.80 | 82 | 98 |
| | *2.611* | *2.432* | *1.796* | *82.1* | *97.5* |
| Pb, Bu$^t$ | 2.68 | 2.48 | 1.80 | 81 | 98 |
| | *2.704* | *2.544* | *1.805* | *82.9* | *96.7* |

The dianion $[P_2C_2H_2]^{2-}$ has $D_{2h}$ symmetry in the ground state with an aromatic sextet of electrons. In the complexes the ring has equal P−C distances and is nearly planar; therefore, the ligand orbitals are referred to by their $D_{2h}$ group labels.

The $P_2C_2H_2$ ring in $D_{2h}$ symmetry has the orbital structure given in Figure 1. The *z*-axis is taken to lie perpendicular to the ring, the C and H atoms lie in the *xz*-plane and the P atoms in the *yz*-plane. The highest occupied orbital, $1b_{3g}$, is P p$\pi$ in character, and the C p$\pi$ orbital, $1b_{2g}$, is more stable. This is closely followed by $2b_{2u}$, which is part of the $\sigma$ structure, is largely localized on the P atoms, and is antibonding across the ring. Deeper lying orbitals of interest are $1b_{1u}$, the most stable ring $\pi$ orbital, and $3a_g$, which has P$\sigma$ character and is bonding across the ring. Isosurfaces for these five orbitals are given in Figure 1. The P "lone pairs" are described by the $3a_g$ and $2b_{2u}$ orbitals.

On interaction with a group 14 atom the symmetry is lowered to $C_{2v}$, so the symmetry distinction between ring $\sigma$ and $\pi$ orbitals is lost. The P localized orbitals, $1b_{3g}$ and $2b_{2u}$, which lie close in energy, both become $b_2$

(15) Baerends, E. J. *ADF*, 2000.02 ed.; Department of Theoretical Chemistry, Vrije Universiteit: Amsterdam, 2000.
(16) van Lenthe, E.; Snijders, J. G.; Baerends, E. J. *J. Chem. Phys.* **1996**, *105*, 6505.
(17) van Lenthe, E.; van Leeuwen, R.; Baerends, E. J.; Snijders, J. G. *Int. J. Quantum Chem.* **1996**, *57*, 281.
(18) Vosko, S. H.; Wilk, L.; Nusair, M. *Can. J. Phys.* **1990**, *58*, 1200.
(19) Becke, A. D. *Phys. Rev.* **1988**, *A38*, 2398.
(20) Perdew, J. *Phys. Rev.* **1986**, *B33*, 8822.

**Table 2. Vertical Ionization Energies (eV) and Relative Band Intensities for M($\eta$-$P_2C_2Bu^t_2$)**

| M = | $A_1$ | $A_2$ | B | C | $D_1$ | $D_2$ | E | F | G | H | I | J |
|---|---|---|---|---|---|---|---|---|---|---|---|---|
| Ge | 8.03 | 8.34 | 8.81 | 9.43 | 10.2 | 10.5 | 10.9 | 11.5 | 12.6 | 13.4 | 14.7 | 15.9 |
| He I | 1 | 0.84 | 0.62 | 0.36 | | | | | | | | |
| He II | 1 | 0.94 | 0.37 | 0.55 | | | | | | | | |
| Sn | 7.69 | 8.00 | 8.36 | 9.32 | 10.1 | 10.4 | 10.7 | 11.4 | 12.6 | 13.4 | 14.7 | 15.7 |
| He I | 1 | 0.79 | 0.79 | 0.43 | | | | | | | | |
| He II | 1 | 0.50 | 0.53 | 0.79 | | | | | | | | |

in symmetry, as is the M $p_y$ orbital. The resultant occupied orbitals, $3b_2$ and $2b_2$, have both ring $\sigma$ and $\pi$ character and may be regarded as linear combinations of a P lone pair orbital and a metal ring bonding orbital. The C p$\pi$ orbital, $1b_{2g}$, interacts with the M $p_x$ orbital to form the $3b_1$ orbital. This is calculated to be the most stable of the three top occupied MOs in all the complexes, although their energies all lie within 0.5 eV of each other. All these interactions, of the $\pi$ type with respect to the metal ring axis, are bonding.

The other significant interactions between metal and ring take place among the $a_1$ set of orbitals. The principal contributors are the $1b_{1u}$ orbital from the ring and the s and $p_z$ orbitals from the metal. The fourth occupied orbital in the complex, $5a_1$, is what might be termed the metal "lone pair". It is composed of an sp hybrid on the metal directed away from the ring and the ring $1b_{1u}$ orbital. It is effectively nonbonding. The bonding counterpart is the $3a_1$ orbital. This has metal s character, but little metal $p_z$ character. The $4a_1$ orbital is metal ring nonbonding and correlates directly with the P localized ring $3a_g$ orbital.

Comparison of the orbital energies shows an irregular trend among the $a_1$ set. Relativistic stabilization is experienced by the 6s electrons of the elements occurring after the third transition series; thus the $a_1$ orbitals in Pb($\eta^4$-$P_2C_2H_2$) with Pb 6s character are lower in energy than the corresponding Sn($\eta^4$-$P_2C_2H_2$) ones. Otherwise there is a general increase in orbital energy on descending the group.

**Photoelectron Spectroscopy.** The PE spectra of M($\eta^4$-$P_2C_2Bu^t_2$), where M is Ge and Sn, are presented in Figures 2 and 3. IEs of key features are given in Table 2 together with relative band intensities for the first four bands. Pb($\eta^4$-$P_2C_2Bu^t_2$) was judged to be too thermally unstable for spectral acquisition.

The ionization region between 10 and 18 eV is dominated by the $Bu^t$ groups. Below 10 eV at least four spectral bands can be identified. Gaussian fitting of the He I spectral band areas gave peaks of equal widths to $A_1$, $A_2$, and C with B slightly broader. However $A_1$ and $A_2$ overlap sufficiently for a range of relative areas to give reasonable fits. In both cases $A_1$ is the most intense of the four bands in both the He I and He II spectra. In the He II spectra B decreases in intensity relative to $A_1$ for both Ge and Sn; C increases in intensity relative to $A_1$ for both metals. For Ge, $A_2$ increases in intensity relative to $A_1$ with an increase in photon energy, whereas the opposite is the case for Sn.

These intensity increases can give an indication of the origin of the spectral bands. Theoretical calculations of the cross section variations of the relevant atomic orbitals are given in Figure 4. [21] These calculations give

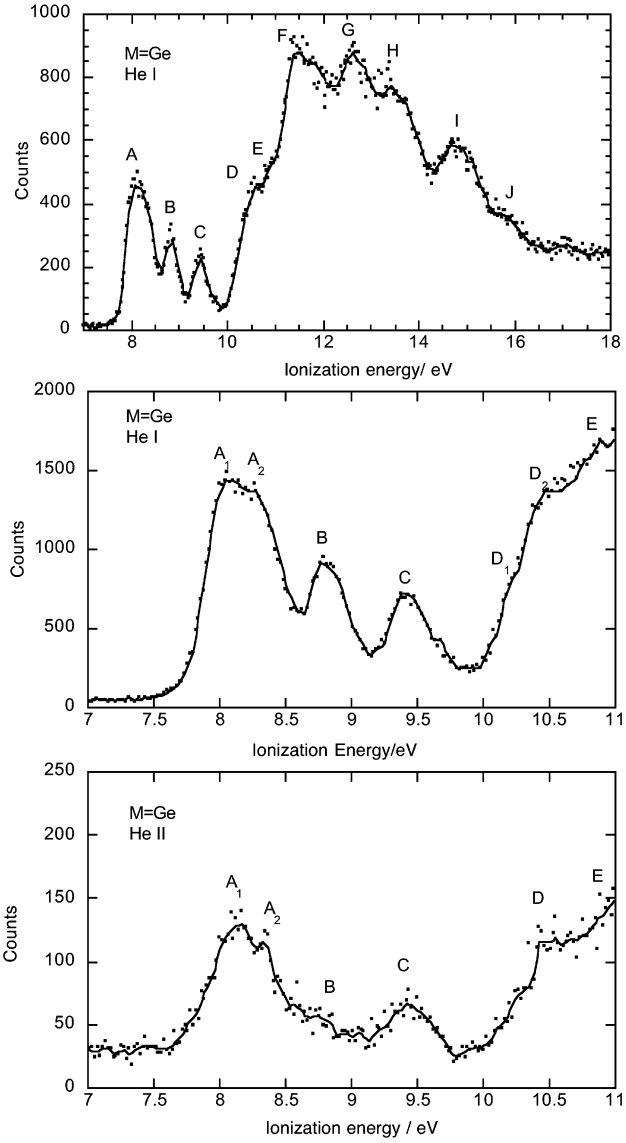


**Figure 2.** He I and He II PE spectra of Ge($\eta^4$-$P_2C_2H_2$).

a good guide as to how the cross sections change with photon energy, although the absolute values are not always reliable. C 2p ionizations are the most intense between 20 and 45 eV. Both Ge and Sn ns cross sections are low at He I photon energies but are relatively higher at He II photon energies. P, Ge, and Sn all have nodes in their np orbitals which lead to Cooper minima between 30 and 50 eV. Thus their ionization bands are found experimentally to lose intensity relative to C 2p ionizations between He I and He II spectra. Taking these trends into consideration, it seems reasonable to assign band C to the $5a_1$ orbital, which has M ns character, band B to the $2b_2$ orbital because of its P character, and for Sn, bands $A_1$ and $A_2$ to the $3b_1$ and $3b_2$ orbitals, respectively. For Ge the high intensity of

(21) Yeh, J.-J. *Atomic calculation of photoionization cross-sections and asymmetry parameters*; Gordon and Breach Science Publishers: Langhorne, 1993.

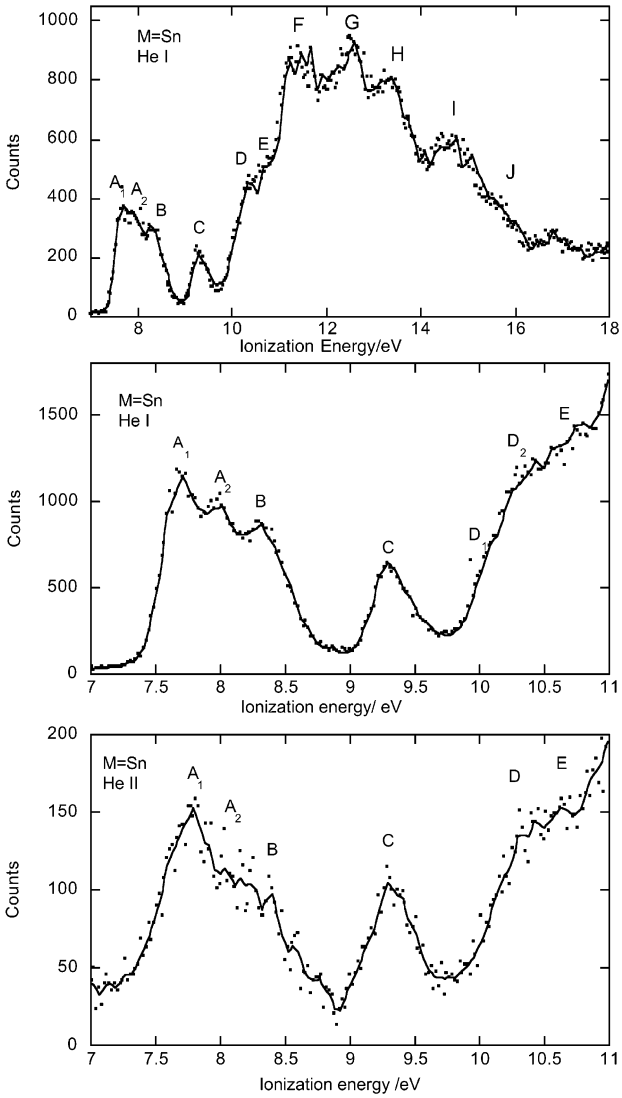


**Figure 3.** He I and He II PE spectra of Sn($\eta^4$-$P_2C_2H_2$).

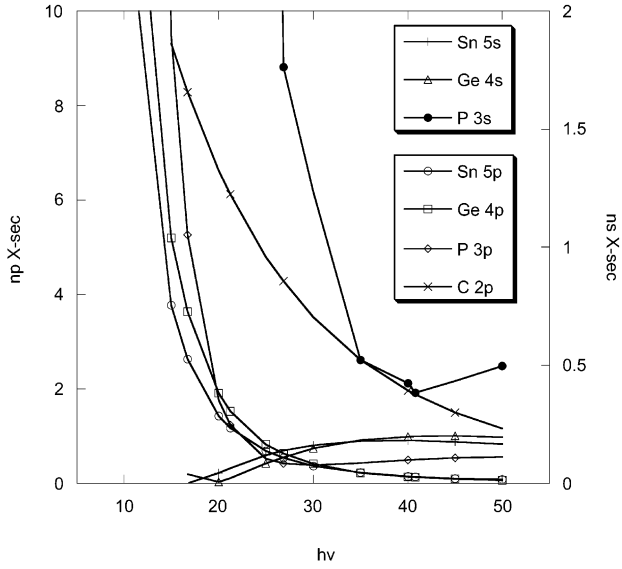


**Figure 4.** Computed cross sections for the atomic orbitals C 2p, P 3p, Ge 4s and 4p, and Sn 5s and 5p.

$A_1$ in the He I spectrum indicates its C 2p character; hence it is also likely to arise from the $3b_1$ orbital, but the fact that it appears to lose intensity relative to $A_2$ in the He II spectrum could indicate P 3p character and a $2b_2$ origin.

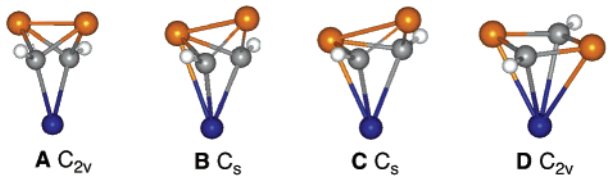


**Figure 5.** Stationary points, **A**−**D**, found for M($\eta^4$-$P_2C_2H_2$) showing a possible rearrangement pathway. **A** and **C** represent transition states and **B** and **D** local minima.

**Table 3. Orbital Energies and Experimental and Calculated IEs (eV) for M($\eta$-$P_2C_2Bu^t_2$)**

| | Ge | | | Sn | | |
|---|---|---|---|---|---|---|
| orbital | energy | IE calc | IE exptl | energy | IE calc | IE exptl |
| $3b_2$ | −5.49 | 7.80 | 8.34 $A_2$ | −5.30 | 7.59 | 8.00 $A_2$ |
| $3b_1$ | −5.58 | 7.75 | 8.03 $A_1$ | −5.35 | 7.49 | 7.69 $A_1$ |
| $2b_2$ | −6.13 | 8.49 | 8.81 B | −5.83 | 8.14 | 8.36 B |
| $5a_1$ | −7.05 | 9.25 | 9.43 C | −6.91 | 9.12 | 9.32 C |

Further help with the assignment is possible by using DFT to calculate the IEs. The results are given in Table 3 together with the orbital energies from the ground state calculation. These calculations confirm that only four bands are expected in the low IE region. Overall the calculated IEs are close to the experimental values but consistently too low. The calculations agree with experiment in giving lower IE values for Sn($\eta^4$-$P_2C_2Bu^t_2$) than for Ge($\eta^4$-$P_2C_2Bu^t_2$). For both Ge and Sn the IE ordering calculated is $3b_1 < 3b_2 < 2b_2 < 5a_1$. This ordering is consistent with the intensity data. It is noteworthy that there is a Koopmans' type of order change between the orbital energies and the IE. The $3b_1$ orbital is the second highest occupied orbital in the complexes but has the lowest IE. In the unsubstituted model compounds it was the third highest orbital, but substitution by the $Bu^t$ groups destabilizes this largely C-based orbital more than the $3b_2$ and $2b_2$ orbitals, which are P-based.

**Rearrangement) to M($\eta^4$-$P_2C_2H_2$).** It is of interest to model the structure of a possible intermediate in the formation of M($\eta^4$-$P_2C_2H_2$) by direct transfer of the 1,3-diphosphabicyclo[1.1.0]butane ligand from the Zr precursor to the group 14 metal. Exploration of the energy surface for all three metals leads to characterization of stationary points **A**, **B**, **C**, and **D**. Geometry optimization of A with $C_{2v}$ symmetry led to a stationary point on the energy surface with one imaginary frequency corresponding to motion of M toward the P atoms. Relaxation of the symmetry constraint gave an intermediate **B** in which an M−P bond has formed. **B** has a square-pyramidal framework, with M in the square base and P at the apex; it possesses $C_s$ symmetry, the mirror plane passing through M and the P atoms. Rearrangement of B to D, M($\eta^4$-$P_2C_2H_2$), is energetically favorable. In all cases a transition state, **C**, lying between **B** and **D**, was identified. The energies of these various species for all three metals are given in Table 4. **A** would possess two P lone pairs and an empty M p orbital. It is favorable for the P atoms to tilt toward the metal and form a P−M bond as in **B**. The transition to **D** involves breaking the P−P bond in order to form a further P−M interaction and the delocalized ring; hence it is an

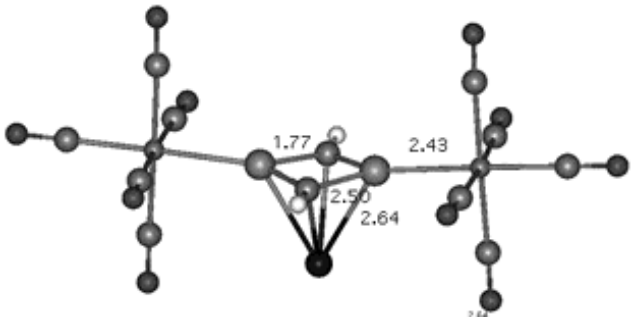


**Figure 6.** Structure calculated for {[Sn($\eta^4$-$P_2C_2H_2$)]-[$W(CO)_5]_2$}.

**Table 4. Relative Energies (kJ mol$^{-1}$) of Stationary Points for M($\eta^4$-$P_2C_2H_2$) (M = Ge, Sn, Pb) and Imaginary Vibrations (cm$^{-1}$) for the Transition States A and C**

| | M | A | B | C | D |
|---|---|---|---|---|---|
| energies | Ge | 95 | 86 | 113 | 0 |
| | Sn | 104 | 97 | 121 | 0 |
| | Pb | 114 | 107 | 130 | 0 |
| imaginary vibrations | Ge | −155*i* | | −365*i* | |
| | Sn | −138*i* | | −407*i* | |
| | Pb | −133*i* | | −403*i* | |

activated process. In the context of cluster chemistry, the greater stability of **D** over **B** is attributed to the desirability of having the most electropositive element at the apex of the square pyramid.

**Reactions of M($\eta^4$-$P_2C_2Bu^t_2$).** The molecules M($\eta^4$-$P_2C_2Bu^t_2$) have shown two types of reactivity.[8] Sn($\eta^4$-$P_2C_2Bu^t_2$) acts as a base, coordinating one or two $W(CO)_5$ groups at the P atoms. This is consistent with the observation that the $3b_2$ orbital, formed from the P lone pairs, is significantly higher in energy than the $5a_1$ orbital, which represents the metal lone pair. Geometry optimization of {[Sn($\eta^4$-$P_2C_2H_2$)][$W(CO)_5]_2$} gave the structure shown in Figure 6.

The Sn−P and Sn−C distances were 2.64 and 2.50 Å, respectively, compared with 2.64 and 2.44 Å in Sn($\eta^4$-$P_2C_2H_2$). The P−C bond was 1.77 Å, slightly shorter than the 1.79 Å calculated for Sn($\eta^4$-$P_2C_2H_2$). Thus the bonding of the ring to Sn is little perturbed by coordinating the two $W(CO)_5$ groups. Most interestingly, the P−P−W angle is 175°; thus the lone pairs to which the W's are coordinating lie more or less in the plane of the ring. Thus the calculated structure confirms that the principal interaction of the ring with the metal is through the ring $\pi$ orbitals and the P lone pairs are not involved.

Ge($\eta^4$-$P_2C_2Bu^t_2$) undergoes oxidative addition by $I_2$ to form Ge($P_2C_2Bu^t_2$)$I_2$, in which the X-ray structure shows the Ge to be bound in a tetrahedral manner solely to the iodines and the two framework carbons, and a P−P bond has been formed. The geometry of Ge($P_2C_2H_2$)$I_2$ was optimized starting from a structure with a planar $\eta^4$ geometry for the $P_2C_2$ ring.

The optimized structure, shown in Figure 7, has $C_{2v}$ symmetry, and a bicyclic, open butterfly structure for the $P_2C_2$unit with a P−P bond. In the reaction, not only is the Ge lone pair utilized in the oxidative addition but

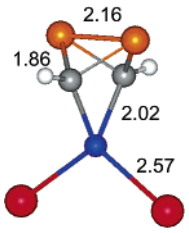


**Figure 7.** Structure calculated for Ge($P_2C_2H_2$)$I_2$.

a Ge p orbital is used in forming the Ge−I bonds so is unavailable for $\eta^4$ coordination by the $P_2C_2$ ring.

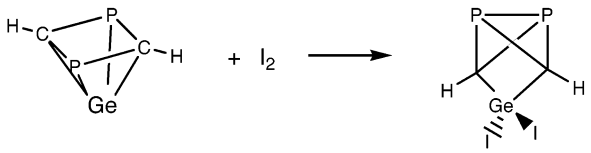


The gas phase reaction was calculated to be exoenergetic by −102 kJ mol$^{-1}$. Values for the corresponding reactions of the Sn and Pb analogues were estimated as −102 and −68 kJ mol$^{-1}$. The alternating energy of the metal lone pair discussed above combined with the decreasing bond strength on descending the group accounts for this irregular trend in reaction energy. The values found suggest that oxidative addition may also be favorable for the Sn and Pb compounds.

## Conclusions

The binding of diphosphacyclobutadiene to a group 14 metal to form M($\eta^4$-$P_2C_2Bu^t_2$) utilizes the three lowest energy $\pi$ orbitals of the ring and three of the valence orbitals of the metal. Bonds of $\pi$ symmetry with respect to the metal ring axis are formed primarily with the ring $1b_{2g}$ and $1b_{3g}$ $\pi$ orbitals and the metal $p_x$ and $p_y$ orbitals; the P $\sigma$ lone pair orbitals make little contribution. The $\sigma$ bonding interaction consists of donation from the ring $1b_{1u}$ $\pi$ orbital into the metal s orbital. The two "metal" electrons are accommodated in a metal ring nonbonding orbital with a metal sp hybrid directed away from the ring mixed with the ring $1b_{1u}$ orbital. Details of the energy scheme are confirmed by the PE spectra of Ge($\eta^4$-$P_2C_2Bu^t_2$) and Sn($\eta^4$-$P_2C_2Bu^t_2$).

A possible intermediate in the formation of M($\eta^4$-$P_2C_2$-$Bu^t_2$) is identified as having a square-pyramidal framework with the metal in the base and P at the apex.

Modeling of the acid−base adduct {[Sn($\eta^4$-$P_2C_2H_2$)]-[$W(CO)_5]_2$} suggests that the P lone pairs are little utilized in metal ring bonding.

The oxidative addition of $I_2$ to M($\eta^4$-$P_2C_2H_2$) is shown to be equally favorable for Ge and Sn but less so for Pb and involves the spontaneous rearrangement to the bicyclic form of the $P_2C_2H_2$ ligand with formation of a P−P bond.

**Acknowledgment.** We thank the EPSRC for a studentship (G.A.). Part of this work was carried out using the facilities of the Oxford Super-computing Centre and part using the EPSRC Columbus Cluster at the Rutherford Laboratory.

OM030161M